

# Latent Neural Stochastic Differential Equations for Change Point Detection

Artem Ryzhikov<sup>a</sup>, Mikhail Hushchyn<sup>a</sup> and Denis Derkach<sup>a</sup>

<sup>a</sup>HSE University, 11 Pokrovsky Bulvar, Moscow, 101000, Russia

---

## ARTICLE INFO

**Keywords:**

Machine Learning  
Deep Learning  
Anomaly Detection  
Change Point Detection  
Timeseries

---

## ABSTRACT

The purpose of change point detection algorithms is to locate an abrupt change in the time evolution of a process. In this paper, we introduce an application of latent neural stochastic differential equations for change point detection problem. We demonstrate the detection capabilities and performance of our model on a range of synthetic and real-world datasets and benchmarks. Most of the studied scenarios show that the proposed algorithm outperforms the state-of-the-art algorithms. We also discuss the strengths and limitations of this approach and indicate directions for further improvements.

---

## 1. Introduction

Change points correspond to abrupt alternations in time series behavior. The presence of such points signals significant changes in processes inside the system under study due to various endogenous and exogenous reasons. Change points detection (CPD) arises in many applications such as production quality control [1], chemical process control [2], detection of climate changes [3], human motion and health state analysis [4], aircraft monitoring [5], vibration monitoring of mechanical systems [6], seismic signal processing [7], detection of cyberattacks [8], video scene analysis [9], audio signal segmentation [10], and many others [11].

Behavior of a variety of systems in biology, physics, engineering, and finance is governed by stochastic processes [12]. One of the important problems is to find Stochastic Differential Equations (SDE) that model these processes. In this work, we use deep neural networks to learn a Latent SDE [13, 14] which approximates the time series. The proposed method provides fitting time series dynamics, where the continuous flow is described by a Latent SDE [13, 14]. In previous works [15, 16], SDE is applied to a limited set of change points and uses a strictly limited parametric set of drift and diffusion functions. In contrast, we develop a scalable unsupervised CPD algorithm that uses a full power of deep learning to approximate the SDE solution with no limitations on kernels, parameters space, and change point types. We evaluate performance of the algorithm on TCPD [17], SKAB [18], TEP [19], and TSSB [20] open CPD benchmarks, and compare the results with the available state-of-the-art methods.

This work has the following structure. Section 2 gives the problem statement, describes related works, and presents Latent SDE fit using deep neural networks. The proposed change point detection algorithm and data processing are described in Section 3. Section 4 defines the quality metrics that we use to compare our method with others. The experimental results and their discussion are provided in Sections 5 and 6 respectively. Finally, conclusion with the main results of this work is presented in Section 7.

## 2. Background, motivation and challenges

This section contains the CPD problem statement along with the existing CPD methods overview. We also provide here all necessary background information for our work, including Latent SDE inference framework.

---

 aryzhikov@hse.ru (A. Ryzhikov); mhushchyn@hse.ru (M. Hushchyn); dderkach@hse.ru (D. Derkach)  
 <https://www.hse.ru/en/org/persons/190912317> (A. Ryzhikov); <https://www.hse.ru/en/org/persons/213369348> (M. Hushchyn); <https://www.hse.ru/en/org/persons/148813333> (D. Derkach)  
ORCID(s): 0000-0002-3543-0313 (A. Ryzhikov); 0000-0002-8894-6292 (M. Hushchyn); 0000-0001-5871-0628 (D. Derkach)  
 <https://www.linkedin.com/profile/view?id=artem-ryzhikov-2b6308103> (A. Ryzhikov), <https://www.linkedin.com/profile/view?id=AAMAAAEV0coBGneke2k10-Pvkvfmw2JJ21d4jiE> (D. Derkach)

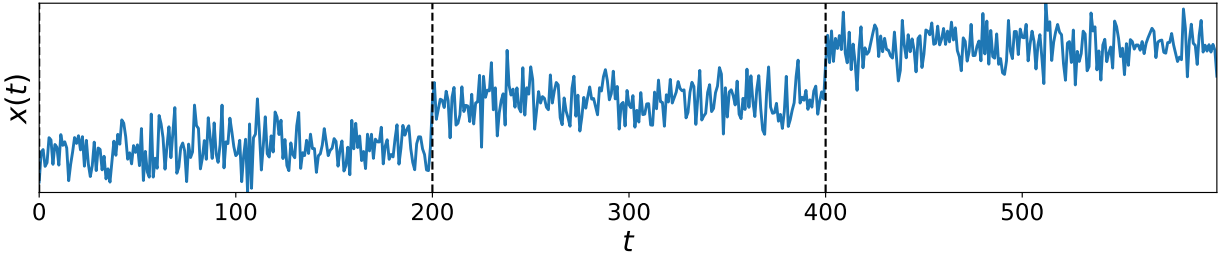


**Figure 1:** Example of a time series with two change points at times  $v_1 = 200$  and  $v_2 = 400$ . At these moments, the mean value of the signal changes with jumps.

## 2.1. Problem statement

Consider a  $d$ -dimensional time series, where each observation at a moment  $t$  is described by a vector of features  $x_t \in \mathbb{R}^d$ :

$$X = \{x_1, x_2, x_3, \dots, x_v, x_{v+1}, x_{v+2}, \dots\}$$

We assume that distribution of all observations with  $t < v$  are sampled from distribution  $P$ , and distribution of all observations with  $v \leq t$  are sampled from distribution  $Q \neq P$ . A moment  $v \geq 1$  when the distribution changes is called a change point. In other words, the change point is a moment when a time series changes its behavior. The illustration of several change-points is demonstrated in Fig. 1. The goal is to detect all change points in time series data. Usually, this is an unsupervised problem in statistics and machine learning due to the absence of true positions of such points.

## 2.2. Related work

Change point detection (CPD) is a long-studied problem. The first works on the change-point detection is dated in the 50s [21, 22] for detecting a shift in the mean value of a signal for quality control of manufacturing processes. In the following decades, a range of change-point detection methods is developed, that can be split between several groups based on cost function, search method, and additional constraints [23].

One of such groups is a set of subspace methods. This line of CPD algorithms is based on the time-series subspace analysis of the original time series, which has a strong connection with a system identification method. This method has been thoroughly studied in the area of control theory [24]. Some subspace methods, like subspace identification (SI) [25] and singular spectrum transformation (SST) [26, 27], are based on classical approaches, for example matrix and SVD transformation of the time series. Some others use more complicated neural network projections to time-invariant subspace [28].

Another common group of change-point detection methods is based on comparison of the empirical probability density distributions before and after change points. CUSUM [22, 29] algorithm assumes that these distributions are known and detects a change point using a sequential hypotheses test procedure. GLR [11, 30] method supposes that parameters of the distribution after the change-point are unknown and estimates it by likelihood minimization. Generally, these methods use hypothesis comparison tests, comparing null and alternative hypothesis likelihoods in each point [31, 32, 33, 34, 35]. Usually [30, 36, 37], null hypothesis suggests that no change points occur in the point, whereas alternative hypothesis suggests that a change point is present in the point.

The next group of methods is based on estimation of some statistics. For instance, a Gaussian process (GP) is a probabilistic method to describe stationary time series analysis and prediction [38]. Another method, called Bayesian Change Point Detection (BCPD) [36], estimates the posterior distribution over an auxiliary variable run length  $r_t$ , which represents the time that elapsed since the last change point. Given the run length at a time instant  $t$ , the run length at the next time point can be either reset back to 0, if a change point occurs at this time, or increased by 1, if the current state continues for one more time unit.

A range of CPD approaches is based on direct probability densities ratio estimation for two samples without the need to know the individual densities [39]. One of the first such algorithms uses logistic regression on RBF kernels [40]. Later, other methods based on RBF kernels were proposed: KLIEP [41], uLSIF [42], and RuLSIF [43]. Their application to change-point detection are described in [24, 44, 45].

Another group of methods also splits the time series into windows and then use a kernel-based statistical test to assess the homogeneity between subsequent windows [46]. One of such recent deep learning kernel-based methods is called KL-CPD [47]. It uses maximum mean discrepancy (MMD) statistical test [48] between distributions  $P$  and  $Q$  of windows before and after the change point respectively (see previous section 2.1).

One more group of CPD methods is based on cost functions [49]. These methods estimate the discrepancy score between two segments of a time series by comparing cost function values before and after splitting the segment into two by a change-point. The most popular algorithms of this group are Binseg [50], Pelt [51, 52], and Window [49].

Graph-based CPD methods first infer a graph by mapping observations (i.e. windows or sets of time series) to nodes and connecting nodes by edges if their pairwise similarity exceeds a predefined threshold. Next, a bespoke graph statistic is applied to split the graph into sub-graphs leading to change points in the time series [53].

From a different perspective, the problem of change point detection can be considered as a clustering problem with a known or unknown number of clusters, such that observations within clusters are identically distributed, and observations between adjacent clusters are not. If a data point at time stamp  $t$  belongs to a different cluster than the data point at time stamp  $t + 1$ , then a change point occurs between the two observations. One of such recently introduced methods is the Classification Score Profile (ClaSP) which performs segmentation of the time series [20] using KNN classification procedure.

In this work, we propose a novel Latent Stochastic Differential Equation's likelihood ratio method for change point detection.

### 2.3. Latent Stochastic Differential Equations

Consider a  $D$ -dimensional time series  $X = \{x_t \in \mathbb{R}^D\}_{t \in \mathbb{T}}$  in time interval  $\mathbb{T} = [0, T]$ ,  $\{w_t\}_{t \in \mathbb{T}}$  is a  $D$ -dimensional Wiener process.

Then, a stochastic process  $\{x_t\}_{t \in \mathbb{T}} \in \mathbb{R}^D$  can be defined by an Itô SDE:

$$dx_t = \mu(x_t, t)dt + \sigma(x_t, t)dw_t, \quad (1)$$

if  $x_0$  is independent of the  $\sigma$ -algebra generated by  $w_t$ , and

$$x_T = x_0 + \int_0^T \mu(x_t, t)dt + \int_0^T \sigma(x_t, t)dw_t, \quad (2)$$

where,  $\mu(x_t, t) : \mathbb{R}^D \times \mathbb{T} \rightarrow \mathbb{R}^D$  is the *drift function*,  $\sigma(x_t, t) : \mathbb{R}^D \times \mathbb{T} \rightarrow \mathbb{R}^D$  is the *diffusion function* and the second integral in (2) is the Itô stochastic integral [54]. When the functions are globally Lipschitz, that is,

$$||\mu(x, t) - \mu(y, t)|| + ||\sigma(x, t) - \sigma(y, t)|| \leq L||x - y|| \quad \forall x, y \in \mathbb{R}^D, t \in \mathbb{T} \quad (3)$$

for some constant  $L > 0$ , there exists a unique  $t$ -continuous strong solution to (1) [54, 13].

In case of high dimension  $D$  of time series  $X$ , a more efficient use of SDE on latent spaces  $\{z_t \in \mathbb{R}^d | d \leq D\}$  can be used [13, 14]. In [14], the authors propose an efficient variational inference framework for such latent SDE models. In particular, given observations  $X$ , they parameterize both a prior over functions and an approximate posterior of latent  $Z$  using SDEs:

$$\begin{aligned} d\tilde{z}_t &= \mu_\theta(\tilde{z}_t, t)dt + \sigma(\tilde{z}_t, t)dw_t, && \text{(prior)} \\ dz_t &= \mu_\phi(z_t, t)dt + \sigma(z_t, t)dw_t, && \text{(approx. posterior)} \\ \tilde{z}_0 &= z_0 \sim \psi(x_0), && \text{(initial latent state)} \\ x_t &= f(z_t), && \text{(decoded states)} \end{aligned}$$

where  $\mu_\theta$ ,  $\mu_\phi$ , and  $\sigma$  are Lipschitz in both arguments.  $\mu_\theta$  is a prior drift function with prior parameters  $\theta$ ,  $\mu_\phi$  is an approximate posterior drift function with variational parameters  $\phi$ ,  $\psi$  is an encoder, and  $f$  is a decoder. In such a setting, the evidence lower bound (ELBO) can be written [14] as:

$$\log p(x_1, x_2, \dots, x_N | \theta) \geq \mathbb{E}_{z_t} \left[ \sum_{i=1}^N \log p(x_{t_i} | z_{t_i}) - \int_0^T \frac{1}{2} |\mu(z_t, t)|^2 dt \right], \quad (4)$$

where  $u(z_t, t) : \mathbb{R}^d \times \mathbb{R} \rightarrow \mathbb{R}^d$  is:

$$u(z_t, t) = \frac{\mu_\theta(z_t, t) - \mu_\phi(z_t, t)}{\sigma(z_t, t)}, \quad (5)$$

where the expectation is taken over the approximate posterior process defined by (approx. posterior).  $u(z_t, t)$  can be considered as a Kullback–Leibler (KL) divergence between the approximate posterior and prior, which regularizes when the approximate posterior is far from the prior at a point  $(z_t, t)$ . The likelihoods of observations  $x_1, \dots, x_N$  at times  $t_1, \dots, t_N$  depend only on latent states  $z_t$  at corresponding times and a predefined likelihood function  $p(x_t | z_t)$ . In practice, this function is set [13] as a Gaussian distribution:

$$p(x_t | z_t) = \mathcal{N}(x_t | f(z_t), C), \quad (6)$$

where  $f$  is the decoder,  $\mathcal{N}(x_t | f(z_t), C)$  is a p.d.f. of Gaussian distribution with mean  $f(z_t)$  and diagonal variance matrix  $C$ .

## 2.4. Change point detection using SDE

In [15], the authors propose the following SDE model of volatility change point:

$$dx_t = \mu(x_t)dt + \theta_t \sigma(x_t)dw_t \quad (7)$$

and find a time  $v$  when the diffusion coefficient  $\theta_{v-1} \neq \theta_v$  is changed. However, one of the main limitations of the method is that volatility may have more complicated kind of change than up to a multiplier  $\theta$ .

In [16], a more complicated volatility change point model is used:

$$dx_t = \mu(x_t)dt + \sigma(x_t; \theta)dw_t \quad (8)$$

Here, the time when the diffusion parameter  $\theta$  is changed is also considered as a change point.

However, the aforementioned CPD algorithms [15, 16] still have a set of limitations. In first, they are designed to detect volatility change points only. In second, they are strictly limited with a set of drift and diffusion functions  $\mu(\cdot)$ , and  $\sigma(\cdot; \theta)$ .

For instance, in [55] the drift and diffusion functions have the following forms:

$$\mu(x) = (2 - x) \quad (9)$$

$$\sigma(x; \theta) = \theta \quad (10)$$

In [56], the forms are following:

$$\mu(x) = x \quad (11)$$

$$\sigma(x; \theta) = (1 + x^2)^\theta \quad (12)$$

## 3. Proposed Method

In contrast to the previous works [15, 16], we propose new CPD method based on Latent SDE which approximates drift and diffusion functions with arbitrarily neural networks. The proposed method is aimed to find different types of change points in an arbitrarily multivariate time series with unknown drift and diffusion functions.

In the following section, we describe the proposed algorithm with all the related preprocessing and post-processing stages.

### 3.1. Preprocessing

First, the original time series is preprocessed with a standard scaling technique. Very often, a time series has a trend and seasonality, and its observations  $x_i$  can be autocorrelated. In some cases, these properties can complicate the detection of change points. To remove the trend and autocorrelation, we use the SARIMAX [57] model implemented in the Statmodels [58] package. We fit the model for the whole time series with the (5, 1, 0) order of AR parameters, differences, and MA parameters respectively. The prediction of the model for a time moment  $i$  is denoted as  $x_i^{SARIMAX}$ . Residuals of the predictions  $r_i$  are used for further analysis and are estimated as

$$r_i = x_i - x_i^{SARIMAX}. \quad (13)$$

In this work, we optionally use this preprocessing as a hyperparameter of our model for each dataset (13). Also, the positional encoding features are passed as input instead of time  $t$  [59].

### 3.2. Postprocessing

The output of our algorithm is multidimensional, containing the scores for all the original and auxiliary dimensions from the previous section 3.1. In the post-processing stage, we use max aggregation over all the dimensions. That choice of aggregation is justified by the fact that change point in one dimension denotes change point of all the time series, and the most likely dimension change point at each time is taken.

Also, we use prominence post-processing [28] to remove the duplicated peaks around the top one.

### 3.3. Algorithm

In this work, we present a novel likelihood-ratio CPD method based on latent stochastic differential equations. We use the following criterion of change point for our algorithm:

$$CPD(x_t) = \sum_{l=1}^L \log \left( \frac{p(x_t|t)}{p(x_t|t-l)} \right), \quad (14)$$

where  $p(x|t)$  is a probability to observe  $x$  at time point  $t$ , and  $L$  is a time lags range, which is considered as a hyperparameter of the algorithm. To estimate the conditional likelihood  $p(x_t|v)$ , we use the following Monte-Carlo approximation:

$$p(x_t|v) = \int p(x_t|z_v, v)p(z_v|v)dz \quad (15)$$

$$= \mathbb{E}_{z_v \sim p(z_v|v)} p(x_t|z_v, v) \quad (16)$$

$$\approx \frac{1}{N} \sum_{i=1}^N p(x_t|z_v^i, v), \quad (17)$$

where  $N$  trajectories  $z_v^i \sim p(z_v|v)$  are sampled from the pretrained latent SDE model [14]. The SDE dynamics of latent  $Z = \{z_t\}$  is approximated by maximizing the ELBO (4) described in the previous section. If latent trajectories  $z_v^i$  are complex enough, the likelihood function becomes  $p(x_t|z_v^i, v) \approx p(x_t|z_v^i)$ , and can be defined as in (6). So, we use the following form of CPD score at each point  $x_t$ :

$$CPD(x_t) = \sum_{l=1}^L \log \left( \frac{p(x_t|t)}{p(x_t|t-l)} \right) \approx \sum_{l=1}^L \log \left( \frac{\sum_{i=1}^N \mathcal{N}(x_t|f(z_v^i), C)}{\sum_{i=1}^N \mathcal{N}(x_t|f(z_{t-l}^i), C)} \right), \quad (18)$$

where  $f$  is a decoder,  $L = 5$  (lags range) and  $C = 0.1 \cdot I$  (diagonal prior variance matrix) are hyperparameters. The final algorithm is shown in Algorithm 1.

**Algorithm 1** Change point detection with Latent SDE

**Input:**  $D$ -dimensional time series of observations  $X = \{x_t \in \mathbb{R}^D\}_{t=0}^{T-1}$  at times  $T = \{t_i\}_{i=0}^{T-1}$  respectively, Variational encoder  $\psi$  and decoder  $f$  with parameters  $\Theta_\psi$  and  $\Theta_f$  respectively, diffusion function  $\sigma_p(z, t)$  with parameters  $p$ , prior drift function  $\mu_\theta(z, t) = -z$ , approximate posterior drift function  $\mu_\phi(z, t)$  with parameters  $\phi$ , number of epochs  $K$ , learning rate  $\eta$ , lags range  $L$ , and prior variance  $C$ , SARIMA preprocessing option,  $PE$  is a positional encoder,  $N$  is a number of trajectories to sample

```

1:  $X = StandardScaling(X)$ 
2: if SARIMA then
3:    $R = X - (X)^{SARIMAX}$ 
4:    $X = \{X, R\}$  ▷ Add SARIMA residuals feature(s)
5: end if
6: for epoch = 1, ..., K do
7:   Set  $z_t = z_0 + \int_0^t \mu_\phi(z_v, PE(v))dv + \int_0^t \sigma_p(z_v, PE(v))dW_v \Big|_{z_0=\psi(x_0)}$ 
8:
9:   for  $i = 1, \dots, T-1$  do
10:    Set  $u(z_{t_i}) = \frac{\mu_\theta(z_{t_i}, PE(t_i)) - \mu_\phi(z_{t_i}, PE(t_i))}{\sigma_p(z_{t_i}, PE(t_i))}$ 
11:   end for
12:    $Z_t = \{z_{t_i}\}_{i=0}^{T-1}$ 
13:    $\Theta = \{\Theta_\psi, \Theta_f, \phi, p\}$  ▷ Neural networks parameters
14:   Calculate ELBO loss  $\mathcal{L} = \mathbb{E}_{Z_t} \left[ \sum_{i=1}^N \log p(x_{t_i} | z_{t_i}) - \int_0^T \frac{1}{2} |u(z_t)|^2 dt \right]$ 
15:   Update parameters  $\Theta := \Theta + \eta \frac{\partial \mathcal{L}}{\partial \Theta}$  ▷ any other gradient optimization can be used here
16: end for
17: for  $i = 1, \dots, N$  do
18:   Sample latent trajectories  $z^i \sim p(z|X)$ 
19: end for
20: for  $i = 0, \dots, T$  do
21:    $CPD(x_t) = \sum_{l=1}^L \log \left( \frac{\sum_{i=1}^N \mathcal{N}(x_t | z_{t_l}^i, C)}{\sum_{i=1}^N \mathcal{N}(x_t | z_{t-l}^i, C)} \right)$ 
22: end for

```

**Output:** change point scores for observations  $X$

### 3.4. Theoretical properties

In this section, we provide a range of theoretical properties of the proposed algorithm for change point detection. We demonstrate that the  $CPD(x_t)$  score (14) is capable to detect changes of mean, trend, and variance of the given signal. To show that, let's estimate an approximate analytical form of the score, which is defined in Theorem 3.1.

**Theorem 3.1.** Let  $v \in T$  is time moment and  $z_v$  is latent state in time  $v$ . Consider the following normal form of the  $p(f(z_v)|v)$  and  $p(x_t|f(z_v), v)$  distributions:

$$p(f(z_v)|v) = \mathcal{N}(f(z_v)|b_v, \Lambda_v), \quad (19)$$

$$p(x_t|f(z_v), v) = \mathcal{N}(x_t|f(z_v), C). \quad (20)$$

Then, the change point detection score  $CPD(x_t)$  (14) takes the following analytical form:

$$\begin{aligned}
 CPD(x_t) = & \frac{1}{2} \sum_{l=1}^L \left( \log(|C + \Lambda_{t-l}|) + (x_t - b_{t-l})^T (C + \Lambda_{t-l})^{-1} (x_t - b_{t-l}) \right) - \\
 & - \frac{L}{2} \left( \log(|C + \Lambda_t|) + (x_t - b_t)^T (C + \Lambda_t)^{-1} (x_t - b_t) \right)
 \end{aligned} \quad (21)$$

*Proof.* Let's substitute Equations (20) and (19) into the definition of  $p(x_t|\nu)$ . Since  $p(x_t|f(z_\nu), \nu)$  and  $p(f(z_\nu)|\nu)$  are conjugate,  $p(x_t|\nu)$  is also normal:

$$\begin{aligned} p(x_t|\nu) &= \int p(x_t|f(z), \nu)p(f(z)|\nu)df(z) = \\ &= \int \mathcal{N}(x_t|f(z), C) \times \mathcal{N}(f(z)|b_\nu, \Lambda_\nu)df(z) = \\ &= \mathcal{N}(x_t|b_\nu, C + \Lambda_\nu), \end{aligned} \tag{22}$$

$$\log p(x_t|\nu) = -\frac{D}{2} \log(2\pi) - \frac{1}{2} \log(|C + \Lambda_\nu|) - \frac{1}{2}(x_t - b_\nu)^T(C + \Lambda_\nu)^{-1}(x_t - b_\nu). \tag{23}$$

Then, the change point detection score, defined in Equation (14), takes the following form:

$$\begin{aligned} CPD(x_t) &= \sum_{l=1}^L \log \left( \frac{p(x_t|t)}{p(x_t|t-l)} \right) = \\ &= \frac{1}{2} \sum_{l=1}^L \left( \log(|C + \Lambda_{t-l}|) + (x_t - b_{t-l})^T(C + \Lambda_{t-l})^{-1}(x_t - b_{t-l}) \right) - \\ &\quad - \frac{L}{2} \left( \log(|C + \Lambda_t|) + (x_t - b_t)^T(C + \Lambda_t)^{-1}(x_t - b_t) \right) \end{aligned} \tag{24}$$

□

This theorem shows how the change point detection score behaves with different alternations of the signal. We assume, that the mean vector  $b_t$  and the covariance matrix  $C + \Lambda_t$  represent the observed values. Thus, all changes of the time series are reflected in the score values. For simplicity, consider a one-dimension signal, where the score is defined by Corollary 3.1.1.

**Corollary 3.1.1.** *For one-dimensional time series, the change point detection score (24) has the following form:*

$$CPD(x_t) = \frac{1}{2} \sum_{l=1}^L \left( \log(c^2 + \lambda_{t-l}^2) + \frac{(x_t - b_{t-l})^2}{c^2 + \lambda_{t-l}^2} \right) - \frac{L}{2} \left( \log(c^2 + \lambda_t^2) + \frac{(x_t - b_t)^2}{c^2 + \lambda_t^2} \right) \tag{25}$$

where  $\Lambda_\nu = \lambda_\nu^2$  and  $C = c^2$ .

Using Equation (25), let's estimate the behavior of the change point detection score for three popular cases. Consider a one-dimensional time series with a change point at time moment  $t$ . In the first case, we assume, that the mean value of the signal is changed in some time. In the second case, the trend of the signal is changed. Finally, in the third case, the variance of the signal alternates. Corollaries 3.1.2, 3.1.3, and 3.1.4 define the score values for these two change points.

**Corollary 3.1.2.** *Consider a one-dimensional time series with the mean jump  $\Delta b$  at time  $t$ . It means, that,  $\lambda_{t-l} = \lambda_t = \lambda$  and  $b_t \neq b_{t-1} = b_{t-2} = \dots = b_{t-L}$ . Then, the change point detection score  $CPD(x_t)$  has the following form:*

$$CPD(x_t) = \frac{L}{2(c^2 + \lambda^2)}(2x_t - b_t - b_{t-L})(b_t - b_{t-L}). \tag{26}$$

Taking into account that  $\mathbb{E}[x_t] = b_t$ , the following expression is valid:

$$\mathbb{E}[CPD(x_t)] = \frac{L}{2(c^2 + \lambda^2)}(b_t - b_{t-L})^2. \tag{27}$$

**Corollary 3.1.3.** *Consequence of (3.1.2). Consider a one-dimensional time series with the trend jump  $\Delta^2 b$  at time  $t$ . It means, that,  $\lambda_{t-L} = \lambda_t = \lambda$  and  $\Delta b_t \neq \Delta b_{t-1} = \Delta b_{t-2} = \dots = \Delta b_{t-L}$ . Then, the change point detection score  $CPD(\Delta x_t)$  has the following form:*

$$CPD(\Delta x_t) = \frac{L}{2(c^2 + \lambda^2)}(2\Delta x_t - \Delta b_t - \Delta b_{t-L})(\Delta b_t - \Delta b_{t-L}). \quad (28)$$

**Corollary 3.1.4.** *Consider a one-dimensional time series with the variance jump  $\Delta\lambda$  at time  $t$ . It means, that,  $b_{t-L} = b_t = b$  and  $\lambda_t \neq \lambda_{t-1} = \lambda_{t-2} = \dots = \lambda_{t-L}$ . Then, the change point detection score  $CPD(x_t)$  has the following form:*

$$CPD(x_t) = \frac{L}{2} \log \left( \frac{c^2 + \lambda_{t-L}^2}{c^2 + \lambda_t^2} \right) + \frac{L}{2}(x_t - b)^2 \left( \frac{1}{c^2 + \lambda_{t-L}^2} - \frac{1}{c^2 + \lambda_t^2} \right). \quad (29)$$

Taking into account that  $\mathbb{E}[(x_t - b)^2] = c^2 + \lambda_t^2$ , we have the following:

$$\mathbb{E}[CPD(x_t)] = \frac{L}{2} \log \left( \frac{c^2 + \lambda_{t-L}^2}{c^2 + \lambda_t^2} \right) + \frac{L}{2} \left( \frac{c^2 + \lambda_t^2}{c^2 + \lambda_{t-L}^2} - 1 \right). \quad (30)$$

The theorem and corollaries considered in this section provide theoretical foundation for the proposed algorithm. They demonstrate the ability of the algorithm to detect various change points and predict the score values for different cases. Similarly to Corollaries 3.1.2, 3.1.3, and 3.1.4, the theorem helps to estimate the algorithm behavior for any alternation of the observed signal.

## 4. Metrics

Recently, some change point detection benchmarks were introduced: TCPD [17], SKAB [18], TSSB [20], and TEP [19]. In this work, we use four metrics in our experiments: *Covering* [17], *F1* [17], *Relative Change Point Distance (RCPD)* [60, 20], and *NAB* [61], that were presented in the benchmarks. This section is addressed to a detailed explanation of the change point evaluation metrics used in this work.

### 4.1. F1

Consider a time series with several change points. Following [17], we define  $\hat{\mathcal{T}} = \{\hat{\tau}_i\}_m$  as a set of change point locations provided by a detection algorithm and let  $\mathcal{T} = \{\tau_i\}_n$  be a combined set of all human annotations. For a set of ground truth locations  $\mathcal{T}$ , they denote a set of true positives  $TP = \{\tau_i | \exists \hat{\tau}_j : |\hat{\tau}_j - \tau_i| < M\}$ , where  $M = 5$  [17]. That means the algorithm change point prediction can be away from ground truth not farther than  $M$ . We also ensure, that only one  $\hat{\tau}_j$  can be used for a single  $\tau_i$ . The latter requirement is needed to avoid double-counting, and  $M = 5$  is the allowed margin of error. Then, precision (P) and recall (R) are defined as

$$P = \frac{|TP|}{|\hat{\mathcal{T}}|}, \quad R = \frac{|TP|}{|\mathcal{T}|} \quad (31)$$

Then,  $F_1$  is used as a quality measure of change point detection:

$$F_1 = \frac{2PR}{P+R} \quad (32)$$

### 4.2. Covering

The second quality metric is based on a segmentation approach, where each change point is considered as a border between two separate segments of a time series. By analogy with other segmentation tasks, the Jaccard score can be used here:

$$J(\mathcal{A}, \mathcal{A}') = \frac{|\mathcal{A} \cap \mathcal{A}'|}{|\mathcal{A} \cup \mathcal{A}'|}, \quad (33)$$

where  $\mathcal{A}$  is a ground-truth segment and  $\mathcal{A}'$  is a segment formed by the found change points. To expand this metric to a multiple segments case, the authors of [17] propose the *Covering* metric:

$$C(\mathcal{G}, \mathcal{G}') = \frac{1}{T} \sum_{\mathcal{A} \in \mathcal{G}} |\mathcal{A}| \cdot \max_{\mathcal{A}' \in \mathcal{G}'} J(\mathcal{A}, \mathcal{A}'), \quad (34)$$

where  $\mathcal{G}$  and  $\mathcal{G}'$  correspond to ground truth and algorithm segmentation, respectively,  $T$  is a time series length. In the case of multiple annotators, the metric was averaged over the annotators labels.

### 4.3. NAB

The NAB score was introduced in [61] and uses a distance-weighted score for predicted change points within and outside the predefined region around ground truth change points. The region starts at the ground truth position of a change point. Thus, all the change point predictions before the ground truth and all others outside the region are considered as false positives (FP). Within the region, only the nearest prediction is considered as a true positive (TP). All the rest of the predictions within the region are ignored.

For each predicted change point  $\hat{\tau} \in \hat{\mathcal{T}}$ , NAB score is calculated in the following way:

$$\sigma^A(\hat{\tau}) = (A_{TP} - A_{FP}) \left( \frac{1}{1 + e^{5|\hat{\tau} - \tau|}} \right) - 1, \quad (35)$$

where  $|\hat{\tau} - \tau|$  is a relative position of the detected  $\hat{\tau}$  within the region. Here, the profile coefficients  $A = \{A_{TP}, A_{FP}, A_{FN}, A_{TN}\}$  are predefined. In this work, we use 3 different profiles for the evaluation:

$$A_{Standart} = \{A_{TP} = 1.0, A_{FP} = -0.11, A_{FN} = -1.0, A_{TN} = 1.0\}, \quad (36)$$

$$A_{LowFP} = \{A_{TP} = 1.0, A_{FP} = -0.22, A_{FN} = -1.0, A_{TN} = 1.0\}, \quad (37)$$

$$A_{LowFN} = \{A_{TP} = 1.0, A_{FP} = -0.11, A_{FN} = -2.0, A_{TN} = 1.0\}. \quad (38)$$

In our work, NAB score for these three profiles is denoted as NAB.Standart, NAB.LowFP, and NAB.LowFN respectively.

We use default region sizes in NAB scores computation. In [61], the authors show that the region size has a minor impact on the final metric value and is chosen to be in the range from  $\frac{5}{|\mathcal{T}|}\%$  to  $\frac{20}{|\mathcal{T}|}\%$  of the time series length  $T$ . For the predictions  $\hat{\mathcal{T}}$ , the raw score is:

$$S_{\hat{\mathcal{T}}} = \left( \sum_{\hat{\tau} \in \hat{\mathcal{T}}} \sigma^A(\hat{\tau}) \right) + A_{FN} |FN|, \quad (39)$$

where  $|FN|$  is a number of false negatives (empty windows with no detections around the ground truth). Then, the final NAB score for the predictions  $\hat{\mathcal{T}}$  is written in the following rescaled form:

$$NAB_{\hat{\mathcal{T}}} = 100 \frac{S_{\hat{\mathcal{T}}} - S_{\text{null}}}{S_{\text{perf}} - S_{\text{null}}} \quad (40)$$

where  $S_{\text{perf}}$  denotes a raw score for “perfect” detector (one that outputs all true positives and no false positives) and  $S_{\text{null}}$  denotes a raw score for “null” detector (one that outputs no anomaly detections).

### 4.4. Relative Change Point Distance (RCPD)

RCPD was introduced in [60] and later used in the ClaSP change point algorithm [20]. It computes an average distance between the predictions  $\{\hat{\tau} \in \hat{\mathcal{T}}\}$  and nearest change points  $\{\tau \in \mathcal{T}\}$ :

$$RCPD = \frac{1}{T|\hat{\mathcal{T}}|} \sum_{\hat{\tau} \in \hat{\mathcal{T}}} \min_{\tau \in \mathcal{T}} |\tau - \hat{\tau}|, \quad (41)$$

where  $T$  is a time series length regarding the aforementioned notation in the section.

Algorithm	NAB (standard)	NAB (LowFP)	NAB (LowFN)	F1	Covering	RCPD
Perfect detector	100	100	100	1	1	0
<b>SDE</b>	<b>93.68</b>	<b>87.55</b>	<b>95.78</b>	<b>0.88</b>	<b>0.94</b>	<b>0.01</b>
ClaSP	45.98	37.32	49.17	0.7	0.72	0.07
BOCPD	88.69	77.39	92.47	0.53	0.83	0.33
KLCPD	64.3	42.09	74.35	0.7	0.84	0.17
TIRE	80.14	73.98	82.31	0.73	0.79	0.1
WIN	91.73	83.76	94.49	0.83	0.83	0.07
BINSEG	92.25	84.6	94.83	0.76	0.81	0.08
DYNP	91.26	83.23	94.17	0.81	0.8	0.14
KERNEL	91.7	83.72	94.47	0.83	0.81	0.12
Null detector	0	0	0	0	0	$\infty$

**Table 1**

Toy synthetic benchmark (Univariate)

## 5. Experimental Results

In this section, we describe an evaluation of our model along with a comparison of state-of-the-art CPD algorithms like KL-CPD [47], TIRE [28], ClaSP [20], BOCPD [36], BINSEG [62], and *ruptures* [49] algorithms like OPT, KERNEL, and WIN. Each algorithm is evaluated at the best threshold for each quality metric described in the previous section. If the algorithm does not return detection scores, the optimal number of the predicted change points is taken for each metric. Univariate algorithms like ClaSP and BOCPD are evaluated on univariate datasets only. Further, we describe all the evaluation corpuses in detail and provide aggregated results tables over each corpus. A detailed models and hyperparameters setup is described in Appendix A. All other implementation details and datasets are available at our public paper repositories for source code<sup>1</sup> and data<sup>2</sup> respectively.

### 5.1. Our Synthetic Studies

To test the model performance, we first take a simple set of synthetic experiments using artificial datasets. The aim of this synthetic experiment is to check how well our algorithm detects different kinds of change points: trend changes, mean jumps, and volatility changes on univariate and multivariate cases. Each experiment represents noisy data generation with further models quality and robustness estimation.

Figure 3 shows the behavior of the algorithm on 3 simulated change point types: mean, trend, and volatility change points.

The averaged metric values for synthetic corpus are listed in Tables 1,2. For univariate datasets, our algorithm outperforms all the others on all CP metrics. For multivariate datasets, the algorithm outperforms the others on all metrics besides *Low.FN*.

The complete description of the synthetic corpus along with detailed case studies is listed in Appendix B.

### 5.2. Evaluation on Open Datasets

In this section, we evaluate our algorithm and compare it with baselines on open datasets for change point detection: TCPD [17], SKAB [18], TSSB [20], and Tennessee Eastman Process(TEP) [19].

TCPD dataset consists of 37 real time series collected for the change point detection benchmark [17]. It includes 33 univariate and 4 multivariate series with manually labeled change points.

The SKAB corpus contains 35 individual data files. Each file represents a single experiment and contains a single anomaly. The dataset represents a multivariate time series collected from the sensors installed on the testbed [18].

TSSB benchmark consists of 98 univariate datasets: 49 single change point time series, 22 datasets with two change points each, 10 datasets with three change points each, and 11 datasets with 4 change points each [20].

TEP benchmark contains 22 53-dimensional single change point datasets [19].

For univariate and multivariate datasets of the TCPD corpus, the results are shown in Tables 3,4 respectively. The results for the SKAB, TSSB, and TEP corpuses are shown in Tables 5,6,7 respectively.

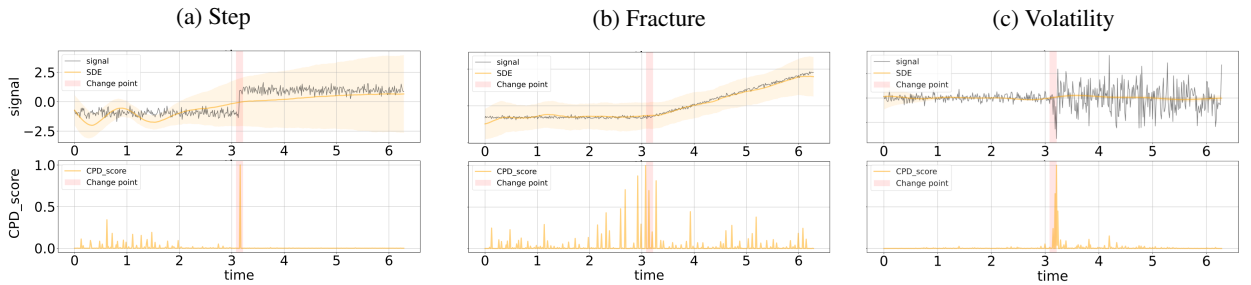
<sup>1</sup><https://gitlab.com/lambda-hse/neural-sde-for-cpd>

<sup>2</sup><https://gitlab.com/lambda-hse/change-point/datasets/>

Algorithm	NAB (standard)	NAB (LowFP)	NAB (LowFN)	F1	Covering	RCPD
Perfect detector	100	100	100	1	1	0
<b>SDE</b>	<b>84.88</b>	<b>79.91</b>	87.05	<b>0.93</b>	<b>0.99</b>	<b>0.01</b>
ClaSP	-	-	-	-	-	-
BOCPD	-	-	-	-	-	-
KLCPD	62.24	47.33	68.82	0.73	0.83	0.23
TIRE	84.66	77.35	87.11	0.76	0.88	0.08
WIN	77.09	55.43	84.72	0.7	0.76	0.25
BINSEG	54.83	45.36	59.88	0.77	0.8	0.18
DYNP	80.8	61.8	87.2	0.73	0.81	0.15
KERNEL	81.51	73.23	84.34	0.8	0.81	0.11
Null detector	0	0	0	0	0	$\infty$

**Table 2**

Toy synthetic benchmark (Multivariate)


**Figure 2: Two pictures**

**Figure 3:** On these figures, the behavior of our algorithm on three main types of change points is shown. On (a), mean change point (step) is shown. On (b), trend change point (fracture) is figured. On (c), volatility change point is shown. The top halves of figures contains original time series with an averaged SDE dynamics. The bottom halves of figures represent the score of our algorithm, maximized over all the original and auxiliary dimensions.

Algorithm	NAB (standard)	NAB (LowFP)	NAB (LowFN)	F1	Covering	RCPD
Perfect detector	100	100	100	1	1	0
<b>SDE</b>	<b>96.43</b>	<b>92.95</b>	<b>97.62</b>	<b>0.77</b>	<b>0.86</b>	<b>0.03</b>
ClaSP	46.45	37.01	52.2	0.34	0.58	0.2
BOCPD	87.81	81.64	91.31	0.45	0.74	0.08
KLCPD	62.79	50	69.95	0.52	0.71	0.15
TIRE	59.55	57.07	63.13	0.46	0.70	0.15
WIN	86.68	80.38	88.99	0.55	0.81	0.12
BINSEG	91.63	84.91	93.96	0.67	0.81	0.06
OPT	90.30	82.29	93.27	0.6	0.72	0.11
KERNEL	88.23	79.19	91.89	0.59	0.73	0.14
Null detector	0	0	0	0	0	$\infty$

**Table 3**

Results on univariate TCPD datasets [17]. Each row (except header) represents the results for a specific algorithm. The first column contains algorithm names. All the rest columns corresponds to specific metrics listed in the header. On each cell, a metric value averaged over all the datasets is shown. The best values for each metric are highlighted in bold.

On the TSSB benchmark, the proposed algorithm outperforms the others only on *F1* score. However, in all the rest studied benchmarks, our algorithm outperforms all other algorithms.

Algorithm	NAB (standard)	NAB (LowFP)	NAB (LowFN)	F1	Covering	RCPD
Perfect detector	100	100	100	1	1	0
<b>SDE</b>	<b>94.29</b>	<b>89.19</b>	<b>96.19</b>	<b>0.66</b>	<b>0.85</b>	<b>0.01</b>
ClaSP	-	-	-	-	-	-
BOCPD	-	-	-	-	-	-
KLCPD	69.79	52.98	78.44	0.4	0.67	0.07
TIRE	63.18	59.91	64.45	0.45	0.63	0.12
WIN	87.77	84.27	89.32	0.55	0.75	0.03
BINSEG	90.08	81.79	92.88	0.56	0.76	0.06
OPT	89.18	81.5	91.79	0.55	0.76	0.06
KERNEL	91.21	84.05	93.63	0.57	0.71	0.05
Null detector	0	0	0	0	0	$\infty$

**Table 4**

Results on multivariate TCPD datasets [17]. Each row (except header) represents the results for a specific algorithm. The first column contains algorithm names. All the rest columns corresponds to specific metrics listed in the header. On each cell, a metric value averaged over all the datasets is shown. The best values for each metric are highlighted in bold.

Algorithm	NAB (standard)	NAB (LowFP)	NAB (LowFN)	F1	Covering	RCPD
Perfect detector	100	100	100	1	1	0
<b>SDE</b>	<b>91.08</b>	<b>84.91</b>	<b>93.54</b>	<b>0.50</b>	<b>0.77</b>	<b>0.05</b>
ClaSP	-	-	-	-	-	-
BOCPD	-	-	-	-	-	-
KLCPD	56.06	40.69	65.17	0.39	0.65	0.14
TIRE	56.45	49.92	63.14	0.41	0.7	0.15
WIN	84.49	72.19	89.41	0.46	0.65	0.12
BINSEG	85.53	73.81	90.02	0.44	0.71	0.10
OPT	83.24	70.08	88.34	0.44	0.68	0.11
KERNEL	85.27	72.97	89.94	0.42	0.61	0.17
Null detector	0	0	0	0	0	$\infty$

**Table 5**

Results on SKAB benchmark datasets [18]. Each row (except header) represents the results for a specific algorithm. The first column contains algorithm names. All the rest columns corresponds to specific metrics listed in the header. On each cell, a metric value averaged over all the datasets is shown. The best values for each metric are highlighted in bold.

## 6. Discussion

Theorem 3.1 and the corresponding corollaries 3.1.1, 3.1.2, 3.1.3, 3.1.4 proves theoretical discriminative power on trend, jump, and volatility change points under certain conditions (19), (20).

The obtained experimental results match well with all the aforementioned theoretical properties of the proposed algorithm. The algorithm effectively detects all the main types of change points and outperforms the existing CPD methods on a wide range of benchmarks. Unlike the previous algorithms, our method shows the best quality both on univariate and multivariate datasets.

We suggest the main reason for such good quality is that our method effectively fits the latent dynamics of a multivariate process with the robust continuous dynamics of SDE. To our knowledge, this is the first approach that effectively utilizes Latent Stochastic Differential Equations for the change point detection task.

Along with a good performance, our algorithm has good flexibility and computing efficiency. The training and inference stages of the algorithm are linear with the respect to time series size  $N$ , whereas lots of other state-of-the-art algorithms with comparably quality are much less scalable, or require much higher computational complexity.

Another main property of our algorithm is flexibility, which helps to use any deep learning based encoder-decoder architectures behind the algorithm. In this work, most of the experiments are conducted on low-dimensional datasets and hence we do not use encoders in our experiments. However, we presume that more detailed study in this direction can additionally improve the existing results of the proposed algorithm in a high-dimensional time series case.

Also, more complicated preprocessing can be used in order to detect seasonality changes.

Algorithm	NAB (standard)	NAB (LowFP)	NAB (LowFN)	F1	Covering	RCPD
Perfect detector	100	100	100	1	1	0
<b>SDE</b>	73.75	61.91	80.2	<b>0.62</b>	0.81	0.08
ClaSP	53.29	46.81	56.22	0.60	0.83	0.02
BOCPD	73.64	58.98	80.24	0.50	0.67	0.22
KLCPD	69.55	55.99	77.26	0.51	0.68	0.24
TIRE	84.11	73.87	87.86	0.54	0.70	0.14
WIN	77.58	63.58	84.42	0.51	0.66	0.17
BINSEG	34.78	24.79	42.95	0.50	0.47	0.32
OPT	62.30	47.83	70.09	0.50	0.63	0.23
KERNEL	65.45	50.34	72.89	0.54	0.69	0.16
Null detector	0	0	0	0	0	$\infty$

**Table 6**

Results on TSSB benchmark datasets [20]. Each row (except header) represents the results for a specific algorithm. The first column contains algorithm names. All the rest columns corresponds to specific metrics listed in the header. On each cell, a metric value averaged over all the datasets is shown. The best values for each metric are highlighted in bold.

Algorithm	NAB (standard)	NAB (LowFP)	NAB (LowFN)	F1	Covering	RCPD
Perfect detector	100	100	100	1	1	0
<b>SDE</b>	<b>94.31</b>	<b>88.62</b>	<b>96.2</b>	<b>0.8</b>	<b>0.97</b>	<b>0.02</b>
ClaSP	-	-	-	-	-	-
BOCPD	-	-	-	-	-	-
KL-CPD	91.2	83.33	94.13	0.67	0.77	0.37
TIRE	58.78	54.65	60.19	0.67	0.72	0.17
BINSEG	91.64	84.59	94.42	0.68	0.8	0.40
OPT	91.71	83.7	94.47	0.69	0.81	0.28
KERNEL	91.71	83.7	94.47	0.69	0.81	0.28
WIN	93.08	86.49	95.38	0.67	0.8	0.35
Null detector	0	0	0	0	0	$\infty$

**Table 7**

Results on Tennessee Eastman Process datasets [19]. Each row (except header) represents the results for a specific algorithm. The first column contains algorithm names. All the rest columns corresponds to specific metrics listed in the header. On each cell, a metric value averaged over all the datasets is shown. The best values for each metric are highlighted with bold.

This way, we first provide and study a general Neural SDE framework in CPD setting, which makes possible to apply a wide range of modern deep learning techniques to CPD problems. This fact, along with all the aforementioned properties, provides a broad perspective for further study and improvements of the proposed algorithm.

## 7. Conclusion

This work was aimed to study Latent SDE in a change point detection setting. It was theoretically and experimentally shown, that the proposed method based on that idea is capable to detect all the main types of change points: trend, mean, and volatility changes. The model shows high robustness and a performance which is higher than other state-of-the-art algorithms in most of the scenarios and metrics. To our knowledge, this is the first studied application of a Neural SDE to change point detection problem, which opens new prospects for further research and DL applications to change point detection task.

## 8. Acknowledgements

The publication was supported by the grant for research centers in the field of AI provided by the Analytical Center for the Government of the Russian Federation (ACRF) in accordance with the agreement on the provision of subsidies (identifier of the agreement 000000D730321P5Q0002) and the agreement with HSE University No. 70-2021-00139.

## References

- [1] A. F. Bissell, Cusum techniques for quality control, *Journal of the Royal Statistical Society. Series C (Applied Statistics)* 18 (1) (1969) 1–30. URL <http://www.jstor.org/stable/2346436>
- [2] B. Huang, Detection of abrupt changes of total least squares models and application in fault detection, *IEEE Transactions on Control Systems Technology* 9 (2) (2001) 357–367. doi:10.1109/87.911387.
- [3] J. Reeves, J. Chen, X. L. Wang, R. Lund, Q. Q. Lu, A review and comparison of changepoint detection techniques for climate data, *Journal of Applied Meteorology and Climatology* 46 (6) (2007) 900–915. arXiv:<https://doi.org/10.1175/JAM2493.1>, doi:10.1175/JAM2493.1. URL <https://doi.org/10.1175/JAM2493.1>
- [4] A. Briassouli, T. Vagia, I. Kompatsiaris, Human motion analysis via statistical motion processing and sequential change detection, *EURASIP Journal on Image and Video Processing* 2009. doi:10.1155/2009/652050.
- [5] D. Henry, S. Simani, R. J. Patton, *Fault Detection and Diagnosis for Aeronautic and Aerospace Missions*, Springer Berlin Heidelberg, Berlin, Heidelberg, 2010, pp. 91–128. doi:10.1007/978-3-642-11690-2\_3. URL [https://doi.org/10.1007/978-3-642-11690-2\\_3](https://doi.org/10.1007/978-3-642-11690-2_3)
- [6] G. A. Susto, A. Schirru, S. Pampuri, S. McLoone, A. Beghi, Machine learning for predictive maintenance: A multiple classifier approach, *IEEE Transactions on Industrial Informatics* 11 (3) (2015) 812–820.
- [7] M. Basseville, I. V. Nikiforov, Detection of abrupt changes: theory and application, *Technometrics* 36 (1993) 550.
- [8] A. G. Tartakovsky, B. Rozovskii, R. B. Blazek, H. Kim, Detection of intrusions in information systems by sequential change-point methods, *Statistical Methodology* 3 (2006) 252–293.
- [9] Z. Gao, G. Lu, C. Lv, P. Yan, Key-frame selection for automatic summarization of surveillance videos: a method of multiple change-point detection, *Machine Vision and Applications* 29. doi:10.1007/s00138-018-0954-7.
- [10] Z. Shuyang, T. Heittola, T. Virtanen, Active learning for sound event detection, *IEEE/ACM Transactions on Audio, Speech, and Language Processing* 28 (2020) 2895–2905.
- [11] A. Tartakovsky, I. Nikiforov, M. Basseville, *Sequential Analysis: Hypothesis Testing and Changepoint Detection*, 2014. doi:10.1201/b17279.
- [12] D. Henderson, P. Plaschko, *Stochastic Differential Equations in Science and Engineering*, WORLD SCIENTIFIC, 2006. arXiv:<https://www.worldscientific.com/doi/pdf/10.1142/5806>, doi:10.1142/5806. URL <https://www.worldscientific.com/doi/abs/10.1142/5806>
- [13] A. Hasan, J. M. Pereira, S. Farsiu, V. Tarokh, Learning latent stochastic differential equations with variational auto-encoders, arXiv preprint arXiv:2007.06075.
- [14] X. Li, T.-K. L. Wong, R. T. Q. Chen, D. Duvenaud, Scalable gradients for stochastic differential equations, *International Conference on Artificial Intelligence and Statistics*.
- [15] M. Kovářík, Volatility change point detection using stochastic differential equations and time series control charts, *International Journal of Mathematical Models and Methods in Applied Sciences*.
- [16] S. M. Iacus, N. Yoshida, Numerical analysis of volatility change point estimators for discretely sampled stochastic differential equations, *Economic Notes* 39 (1-2) (2010) 107–127.
- [17] G. J. J. van den Burg, C. K. I. Williams, An evaluation of change point detection algorithms (2020). arXiv:2003.06222.
- [18] I. D. Katser, V. O. Kozitsin, Skoltech anomaly benchmark (skab), <https://www.kaggle.com/dsv/1693952> (2020). doi:10.34740/KAGGLE/DSV/1693952.
- [19] I. Lomov, M. Lyubimov, I. Makarov, L. E. Zhukov, Fault detection in tennessee eastman process with temporal deep learning models, *Journal of Industrial Information Integration* 23 (2021) 100216.
- [20] P. Schäfer, A. Ermshaus, U. Leser, Clasp-time series segmentation, in: *Proceedings of the 30th ACM International Conference on Information & Knowledge Management*, 2021, pp. 1578–1587.
- [21] M. A. Girshick, H. Rubin, A Bayes Approach to a Quality Control Model, *The Annals of Mathematical Statistics* 23 (1) (1952) 114 – 125. doi:10.1214/aoms/1177729489. URL <https://doi.org/10.1214/aoms/1177729489>
- [22] E. S. Page, Continuous inspection schemes, *Biometrika* 41 (1954) 100–115.
- [23] S. Aminikhahhahi, D. J. Cook, A survey of methods for time series change point detection, *Knowledge and information systems* 51 (2) (2017) 339–367.
- [24] Y. Kawahara, M. Sugiyama, Sequential change-point detection based on direct density-ratio estimation, *Stat. Anal. Data Min.* 5 (2) (2012) 114–127. doi:10.1002/sam.10124. URL <https://doi.org/10.1002/sam.10124>
- [25] Y. Kawahara, T. Yairi, K. Machida, Change-point detection in time-series data based on subspace identification, in: *Seventh IEEE International Conference on Data Mining (ICDM 2007)*, IEEE, 2007, pp. 559–564.
- [26] N. Itoh, J. Kurths, Change-point detection of climate time series by nonparametric method, in: *Proceedings of the world congress on engineering and computer science*, Vol. 1, Citeseer, 2010, pp. 445–448.
- [27] V. Moskvina, A. Zhigljavsky, An algorithm based on singular spectrum analysis for change-point detection, *Communications in Statistics-Simulation and Computation* 32 (2) (2003) 319–352.
- [28] T. D. Ryck, M. de Vos, A. Bertrand, Change point detection in time series data using autoencoders with a time-invariant representation, *IEEE Transactions on Signal Processing* 69 (2021) 3513–3524.
- [29] M. Basseville, I. V. Nikiforov, *Detection of Abrupt Changes: Theory and Application*, Prentice-Hall, Inc., USA, 1993.
- [30] F. Gustafsson, The marginalized likelihood ratio test for detecting abrupt changes, *IEEE Transactions on Automatic Control* 41 (1) (1996) 66–78.

- [31] C. Alippi, G. Boracchi, D. Carrera, M. Roveri, Change detection in multivariate datastreams: Likelihood and detectability loss, arXiv preprint arXiv:1510.04850.
- [32] M. F. R. Chowdhury, S.-A. Selouani, D. O'Shaughnessy, Bayesian on-line spectral change point detection: a soft computing approach for on-line asr, *International Journal of Speech Technology* 15 (1) (2012) 5–23.
- [33] E. Keogh, S. Chu, D. Hart, M. Pazzani, An online algorithm for segmenting time series, in: *Proceedings 2001 IEEE international conference on data mining*, IEEE, 2001, pp. 289–296.
- [34] L. Lacasa, B. Luque, F. Ballesteros, J. Luque, J. C. Nuno, From time series to complex networks: The visibility graph, *Proceedings of the National Academy of Sciences* 105 (13) (2008) 4972–4975.
- [35] R. Malladi, G. P. Kalamangalam, B. Aazhang, Online bayesian change point detection algorithms for segmentation of epileptic activity, in: *2013 Asilomar Conference on Signals, Systems and Computers*, IEEE, 2013, pp. 1833–1837.
- [36] R. P. Adams, D. J. C. MacKay, Bayesian online changepoint detection (2007). [arXiv:0710.3742](https://arxiv.org/abs/0710.3742).
- [37] J. Knoblauch, T. Damoulas, Spatio-temporal bayesian on-line changepoint detection with model selection (2018). [arXiv:1805.05383](https://arxiv.org/abs/1805.05383).
- [38] Y. Saatçι, R. D. Turner, C. E. Rasmussen, Gaussian process change point models, in: *ICML*, 2010.
- [39] M. Sugiyama, T. Suzuki, T. Kanamori, *Density Ratio Estimation in Machine Learning*, Cambridge University Press, 2012. doi:10.1017/CBO9781139035613.
- [40] S. Bickel, M. Brückner, T. Scheffer, Discriminative learning for differing training and test distributions, in: *Proceedings of the 24th International Conference on Machine Learning*, ICML '07, Association for Computing Machinery, New York, NY, USA, 2007, p. 81–88. doi:10.1145/1273496.1273507.  
URL <https://doi.org/10.1145/1273496.1273507>
- [41] M. Sugiyama, S. Nakajima, H. Kashima, P. Buenau, M. Kawanabe, Direct importance estimation with model selection and its application to covariate shift adaptation, in: J. Platt, D. Koller, Y. Singer, S. Roweis (Eds.), *Advances in Neural Information Processing Systems*, Vol. 20, Curran Associates, Inc., 2008.  
URL <https://proceedings.neurips.cc/paper/2007/file/be83ab3ecd0db773eb2dc1b0a17836a1-Paper.pdf>
- [42] T. Kanamori, S. Hido, M. Sugiyama, A least-squares approach to direct importance estimation, *Journal of Machine Learning Research* 10 (48) (2009) 1391–1445.  
URL <http://jmlr.org/papers/v10/kanamori09a.html>
- [43] M. Yamada, T. Suzuki, T. Kanamori, H. Hachiya, M. Sugiyama, Relative density-ratio estimation for robust distribution comparison, *Neural Comput.* 25 (5) (2013) 1324–1370. doi:10.1162/NECO\_a\_00442.  
URL [https://doi.org/10.1162/NECO\\_a\\_00442](https://doi.org/10.1162/NECO_a_00442)
- [44] S. Liu, M. Yamada, N. Collier, M. Sugiyama, Change-point detection in time-series data by relative density-ratio estimation, *Neural Netw.* 43 (2013) 72–83. doi:10.1016/j.neunet.2013.01.012.  
URL <https://doi.org/10.1016/j.neunet.2013.01.012>
- [45] S. Aminikhahhah, T. Wang, D. J. Cook, Real-time change point detection with application to smart home time series data, *IEEE Transactions on Knowledge and Data Engineering* 31 (5) (2019) 1010–1023. doi:10.1109/TKDE.2018.2850347.
- [46] Z. Harchaoui, E. Moulines, F. R. Bach, Kernel change-point analysis, in: *Advances in neural information processing systems*, 2009, pp. 609–616.
- [47] W.-C. Chang, C.-L. Li, Y. Yang, B. Póczos, Kernel change-point detection with auxiliary deep generative models, arXiv preprint arXiv:1901.06077.
- [48] A. Gretton, D. Sejdinovic, H. Strathmann, S. Balakrishnan, M. Pontil, K. Fukumizu, B. K. Sriperumbudur, Optimal kernel choice for large-scale two-sample tests, in: *Advances in neural information processing systems*, Citeseer, 2012, pp. 1205–1213.
- [49] C. Truong, L. Oudre, N. Vayatis, Selective review of offline change point detection methods, *Signal Processing* 167 (2019) 107299. doi:10.1016/j.sigpro.2019.107299.
- [50] P. Fryzlewicz, Wild binary segmentation for multiple change-point detection, *The Annals of Statistics* 42. doi:10.1214/14-AOS1245.
- [51] R. Killick, P. Fearnhead, I. Eckley, Optimal detection of changepoints with a linear computational cost, *Journal of the American Statistical Association* 107 (2012) 1590–1598. doi:10.1080/01621459.2012.737745.
- [52] K. Haynes, I. A. Eckley, P. Fearnhead, Computationally efficient changepoint detection for a range of penalties, *Journal of Computational and Graphical Statistics* 26 (1) (2017) 134–143. [arXiv:https://doi.org/10.1080/10618600.2015.1116445](https://doi.org/10.1080/10618600.2015.1116445), doi:10.1080/10618600.2015.1116445.  
URL <https://doi.org/10.1080/10618600.2015.1116445>
- [53] H. Chen, N. Zhang, Graph-based change-point detection, *The Annals of Statistics* 43 (1) (2015) 139–176.
- [54] L. Arnold, *Stochastic differential equations*, New York.
- [55] O. A. Vasicek, An equilibrium characterization of the term structure, *Journal of Financial Economics* 5 (1977) 177–188.
- [56] Y. Ait-Sahalia, Testing continuous-time models of the spot interest rate, *Research Papers in Economics*.
- [57] J. Durbin, S. J. Koopman, *Time Series Analysis by State Space Methods*, 2nd Edition, Oxford University Press, 2012.  
URL <https://EconPapers.repec.org/RePEc:oxp:obooks:9780199641178>
- [58] S. Seabold, J. Perktold, Statsmodels: Econometric and statistical modeling with python, in: *9th Python in Science Conference*, 2010.
- [59] A. Vaswani, N. Shazeer, N. Parmar, J. Uszkoreit, L. Jones, A. N. Gomez, L. Kaiser, I. Polosukhin, Attention is all you need, *Advances in neural information processing systems* 30.
- [60] S. Gharghabi, Y. Ding, C.-C. M. Yeh, K. Kamgar, L. Ulanova, E. Keogh, Matrix profile viii: domain agnostic online semantic segmentation at superhuman performance levels, in: *2017 IEEE international conference on data mining (ICDM)*, IEEE, 2017, pp. 117–126.
- [61] A. Lavin, S. Ahmad, Evaluating real-time anomaly detection algorithms—the numenta anomaly benchmark, in: *2015 IEEE 14th international conference on machine learning and applications (ICMLA)*, IEEE, 2015, pp. 38–44.

- [62] H. Cho, P. Fryzlewicz, Multiple-change-point detection for high dimensional time series via sparsified binary segmentation, *Journal of the Royal Statistical Society: Series B: Statistical Methodology* (2015) 475–507.

## A. Experiment setup. Train, inference, and implementation details

In this auxiliary section, experimental and training specifics details are described.

In the experiments, each algorithm is used with fixed pre-defined hyperparameters. For BINSEG [62], OPT [49], KERNEL [46], and WIN[49], the best values for hyperparameters obtained by the authors of SKAB benchmark were chosen [18]. For BOCPD [36], ClaSP [20], TIRE [28], KLCPD [47], the best hyperparameters are taken from the corresponding papers.

Neural Stochastic Differential Equation is implemented using `torchsde`<sup>3</sup> framework with `noise_type = diagonal`, `sde_type = Stratonovich_SDE`. The neural SDE networks configuration is shown in Figure 4. In this work, we use `torchsde` configuration as a basis for our one [14].

```
NeuralSDE(
    (approximate posterior drift): DNN(
        (net): Sequential(
            (0): Linear(in_features=n_pos_encodings+2*D, out_features=200, bias=True)
            (1): Tanh()
            (2): Linear(in_features=200, out_features=200, bias=True)
            (3): Tanh()
            (4): Linear(in_features=200, out_features=2*D, bias=True)
        )
    )
    (shared diffusion): 1 (constant)
)
```

**Figure 4:** Architecture of Neural SDE for CPD. In our work, we use 3-layer dense neural network to approximate posterior drift, and constant diffusion (equal to 1 in each point). This configuration is similar to the default configuration in the original neural SDE work [14]. Here,  $D$  denotes the dimensionality of original dataset,  $n\_pos\_encodings$  denotes the number of the added time positional encoding features. Factor 2 before the dimensionality  $D$  means that we augment each time series with SARIMAX residuals of the same dimensionality.

The configuration is trained 100 iterations on each dataset with batch size 512. We monitor the evaluation metrics on each epoch in inference mode and save the best values of it.

For training, we use Adam optimizer with learning rate  $10^{-2}$  and default parameters.

In all the experiments, we use a machine with single 8-core CPU *Xeon E5-2689* and single *Nvidia 1080 Ti* GPU. The training stage for each dataset on that hardware takes approximately 200 minutes.

## B. Synthetic corpus

In our experiments, additional corpus of synthetic datasets is introduced. We make this corpus to see how each algorithm works on different types of change points. To do that, a set of synthetic tests (datasets) is generated for three main types of change points: trend, mean, and volatility change. In Table 8, a complete set of tests is listed. In Tables 9, 10, 11, 12, 13, 14, a detailed results for NAB.Standart, NAB.LowFP, NAB.LowFN, F1, Covering, and RCPD metrics are shown respectively.

<sup>3</sup><https://github.com/google-research/torchsde>

Dataset index	Change point types	Dataset description
1	volatility	Gumbel component is changed (2nd component is Gaussian)
2	volatility	Both Gumbel components are changed
3	volatility	Gumbel component is changed (2nd component is Gumbel)
4	volatility	Covariation of multivariate 2D Gaussian is changed
5	volatility	Single fracture in both components (2D)
6	volatility	2 components of 2D Gaussian noise are changed
7	volatility	1 component of 2D Gaussian noise is changed
8	trend	Single fracture in 1 component (2nd component is flat)
9	trend	Single fracture (1D)
10	trend, jump	Multiple steps and fractures (1D)
11	jump	Single step in 1 component (2nd component is flat)
12	jump	Single step (1D)
13	jump	Single step in both components

**Table 8**

List of synthetic datasets. The first column contains dataset indices. The second column contains types of change points which presents in a dataset. The last column contains detailed dataset description.

Dataset	SDE	ClASP	BOCPD	KLCPD	TIRE	WIN	BINSEG	DYNP	KERNEL
1	<b>94.5</b>	-	-	87.9	94.5	78	17.49	45	94.5
2	0	-	-	27	94.5	45	-5.5	72.5	-5.5
3	<b>94.5</b>	-	-	18.55	75.6	51.12	-5.5	83.5	89
4	93.07	-	-	-5.5	94.5	55.98	-5.5	61.5	89
5	<b>97.12</b>	-	-	60.9	56.61	90.19	91.64	88.9	94.41
6	<b>94.5</b>	-	-	92.3	89	94.5	93.8	94.5	94.5
7	<b>94.5</b>	-	-	75.86	89	91.83	92.21	92.38	86.71
8	<b>97.06</b>	-	-	80.76	94.95	86.25	91.64	91.71	94.46
9	<b>94.5</b>	94.5	89	45	94.5	94.5	94.5	93.07	94.44
10	92.04	48.94	88.08	56.69	74.71	91.7	93.25	91.7	91.67
11	89	-	-	94.5	86.79	89	89	89	89
12	<b>94.5</b>	-5.5	89	91.2	71.2	89	89	89	89
13	<b>94.5</b>	-	-	90.1	71.2	89	89	89	89

**Table 9**

NAB.Stadart metric for synthetic datasets [61]. The first column contains dataset indices. The header contains algorithm names. In cells, NAB.Stadart metric for the corresponding dataset and algorithm is given.

Dataset	SDE	ClASP	BOCPD	KLCPD	TIRE	WIN	BINSEG	DYNP	KERNEL
1	<b>89</b>	-	-	75.8	89	56	-11	-10	89
2	0	-	-	2.6	89	-10	-11	45	-11
3	<b>89</b>	-	-	6.8	71.2	6.63	-11	67	78
4	87.42	-	-	-11	89	11.97	-11	23	78
5	<b>94.35</b>	-	-	21.85	53.3	84.26	83.44	77.89	88.9
6	<b>89</b>	-	-	84.6	78	89	88.23	89	89
7	<b>89</b>	-	-	61.46	78	86.06	86.48	86.67	75.48
8	<b>94.3</b>	-	-	62.01	89.99	74.42	83.44	83.45	88.96
9	<b>89</b>	89	78	5	89	89	89	87.42	88.93
10	84.64	33.97	76.17	38.86	70.55	84.27	<b>86.8</b>	84.27	84.24
11	78	-	-	89	73.59	78	78	78	78
12	<b>89</b>	-11	78	82.4	62.4	78	78	78	78
13	<b>89</b>	-	-	80.2	62.4	78	78	78	78

**Table 10**

NAB.LowFP metric for synthetic datasets [61]. The first column contains dataset indices. The header contains algorithm names. In cells, NAB.LowFP metric for the corresponding dataset and algorithm is given.

Dataset	SDE	ClaSP	BOCPD	KLCPD	TIRE	WIN	BINSEG	DYNP	KERNEL
1	<b>96.33</b>	-	-	91.94	96.33	85.33	44.99	63.33	96.33
2	4.67	-	-	38	96.33	63.33	-3.67	81.67	-3.67
3	<b>96.33</b>	-	-	32.36	77.06	67.41	-3.67	89	92.67
4	95.38	-	-	-3.67	96.33	70.65	-3.67	74.33	92.67
5	<b>98.08</b>	-	-	73.93	57.74	93.46	94.43	92.6	96.27
6	<b>96.33</b>	-	-	94.87	92.67	96.33	95.86	96.33	96.33
7	<b>96.33</b>	-	-	83.91	92.67	94.55	94.81	94.92	91.14
8	<b>98.04</b>	-	-	87.17	96.64	90.83	94.42	94.47	96.31
9	<b>96.33</b>	96.33	92.67	63.33	96.33	96.33	96.33	95.38	96.29
10	94.69	54.85	92.06	65.57	76.47	94.46	95.5	94.46	94.45
11	92.67	-	-	96.33	91.19	92.67	92.67	92.67	92.67
12	<b>96.33</b>	-3.67	92.67	94.13	74.14	92.67	92.67	92.67	92.67
13	<b>96.33</b>	-	-	93.4	74.14	92.67	92.67	92.67	92.67

**Table 11**

NAB.LowFN metric for synthetic datasets [61]. The first column contains dataset indices. The header contains algorithm names. In cells, NAB.LowFN metric for the corresponding dataset and algorithm is given.

Dataset	SDE	ClaSP	BOCPD	KLCPD	TIRE	WIN	BINSEG	DYNP	KERNEL
1	<b>1</b>	-	-	0.93	0.73	0.67	1	1	0.67
2	<b>1</b>	-	-	0.67	0.67	0.67	1	0.67	1
3	<b>0.8</b>	-	-	0.67	0.76	0.67	0.67	0.67	0.67
4	0.67	-	-	0.67	1	0.67	0.67	0.67	0.67
5	<b>1</b>	-	-	0.5	0.5	0.5	0.5	0.5	0.5
6	<b>1</b>	-	-	0.67	0.87	0.67	0.67	0.67	1
7	<b>1</b>	-	-	0.67	0.67	0.67	0.67	0.67	1
8	<b>0.86</b>	-	-	0.5	0.5	0.5	0.5	0.5	0.5
9	0.8	1	0.67	0.67	0.67	0.67	0.67	0.67	0.67
10	<b>0.83</b>	0.44	0.25	0.44	0.6	0.83	0.62	0.77	0.83
11	<b>1</b>	-	-	1	1	1	1	1	1
12	<b>1</b>	0.67	0.67	1	0.93	1	1	1	1
13	<b>1</b>	-	-	1	0.93	1	1	1	1

**Table 12**

F1 metric for synthetic datasets [17]. The first column contains dataset indices. The header contains algorithm names. In cells, F1 metric for the corresponding dataset and algorithm is given.

Dataset	SDE	ClaSP	BOCPD	KLCPD	TIRE	WIN	BINSEG	DYNP	KERNEL
1	<b>0.99</b>	-	-	0.96	0.98	0.94	0.98	0.98	0.72
2	<b>1</b>	-	-	0.79	0.97	0.75	1	0.84	1
3	<b>0.98</b>	-	-	0.76	0.75	0.69	0.92	0.85	0.6
4	0.96	-	-	0.78	0.98	0.62	0.68	0.71	0.59
5	<b>0.99</b>	-	-	0.71	0.58	0.5	0.5	0.64	0.57
6	<b>0.99</b>	-	-	0.76	0.98	0.68	0.87	0.83	0.99
7	0.98	-	-	0.79	0.97	0.69	0.5	0.66	0.99
8	<b>0.98</b>	-	-	0.71	0.64	0.76	0.5	0.59	0.62
9	0.97	0.98	0.8	0.88	0.76	0.68	0.68	0.61	0.59
10	<b>0.86</b>	0.52	0.73	0.62	0.68	0.79	0.74	0.79	0.84
11	<b>1</b>	-	-	0.99	1	1	1	1	1
12	<b>1</b>	-	-	1	0.93	1	1	1	1
13	<b>1</b>	-	-	1	0.93	1	1	1	1

**Table 13**

Covering metric for synthetic datasets [17]. The first column contains dataset indices. The header contains algorithm names. In cells, Covering metric for the corresponding dataset and algorithm is given.

Dataset	SDE	ClaSP	BOCPD	KLCPD	TIRE	WIN	BINSEG	DYNP	KERNEL
1	<b>0.01</b>	-	-	0.07	0.01	0.46	0.01	0.01	0.25
2	0	-	-	0.2	0.01	0.33	0	0.16	0
3	<b>0.01</b>	-	-	0.44	0.26	0.24	0.04	0.08	0.24
4	0.02	-	-	0.35	0.01	0.41	0.41	0.42	0.41
5	<b>0</b>	-	-	0.2	0.21	0.31	0.26	0.07	0.11
6	<b>0</b>	-	-	0.32	0.01	0.21	0.39	0.09	0
7	<b>0.01</b>	-	-	0.5	0.02	0.43	0.42	0.42	0.01
8	<b>0.01</b>	-	-	0.23	0.13	0.09	0.26	0.21	0.08
9	0.02	0.01	0.48	0.5	0.17	0.18	0.18	0.41	0.33
10	0.01	0	0.03	0	0.04	0.02	0.04	0.02	0.02
11	<b>0</b>	-	-	0	0	0	0	0	0
12	<b>0</b>	0.2	0.48	0	0.1	0	0	0	0
13	<b>0</b>	-	-	0	0.1	0	0	0	0

**Table 14**

RCPD metric for synthetic datasets [20]. The first column contains dataset indices. The header contains algorithm names. In cells, RCPD metric for the corresponding dataset and algorithm is given.